

Supplementary Materials: Insight into the Source and Evolution of Oxalic Acid: Characterization of Particulate Organic Diacids in a Mega-City, Shanghai from 2008 to 2020

Ning Zhang ¹, Fan Fan ¹, Yi Feng ¹, Ming Hu ², Qingyan Fu ², Jing Chen ³, Shunyao Wang ^{1,*} and Jialiang Feng ^{1,*}

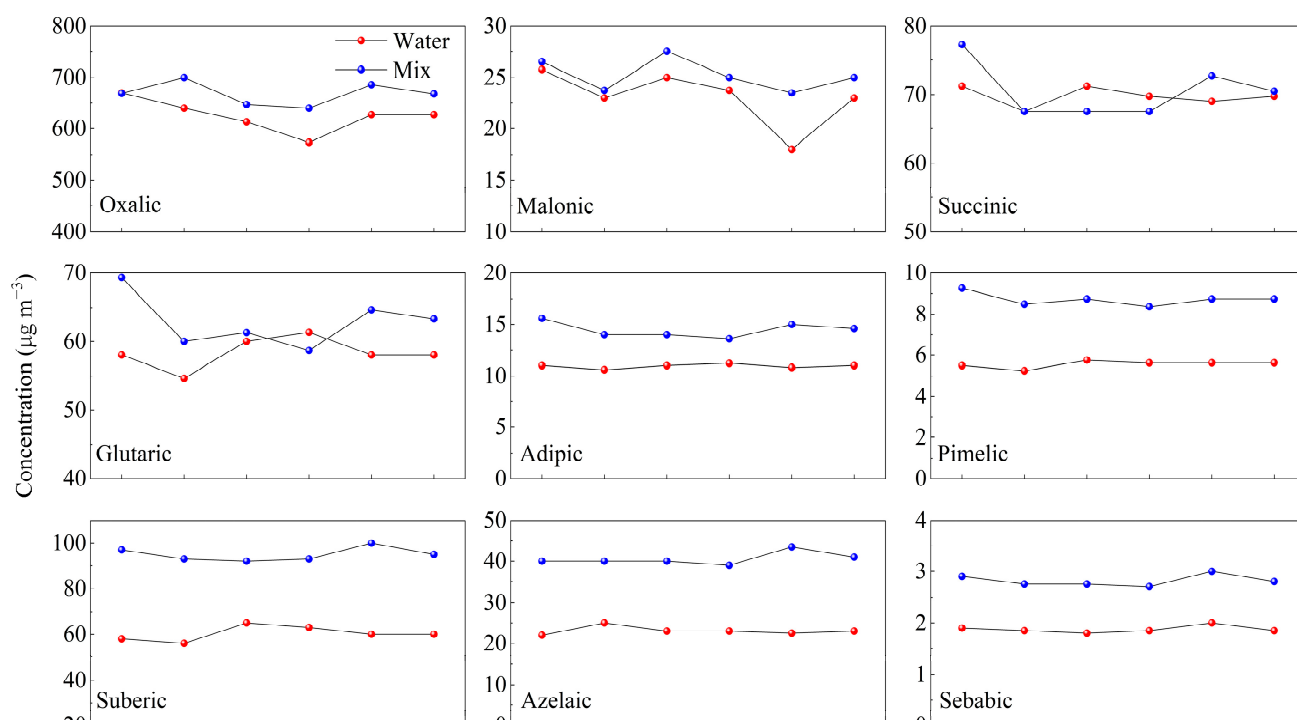


Figure S1. Comparison of the measured concentrations of different diacids in $\text{PM}_{2.5}$ extracted with Water (100% water) and Mix (50% methanol/water solution (v/v)).

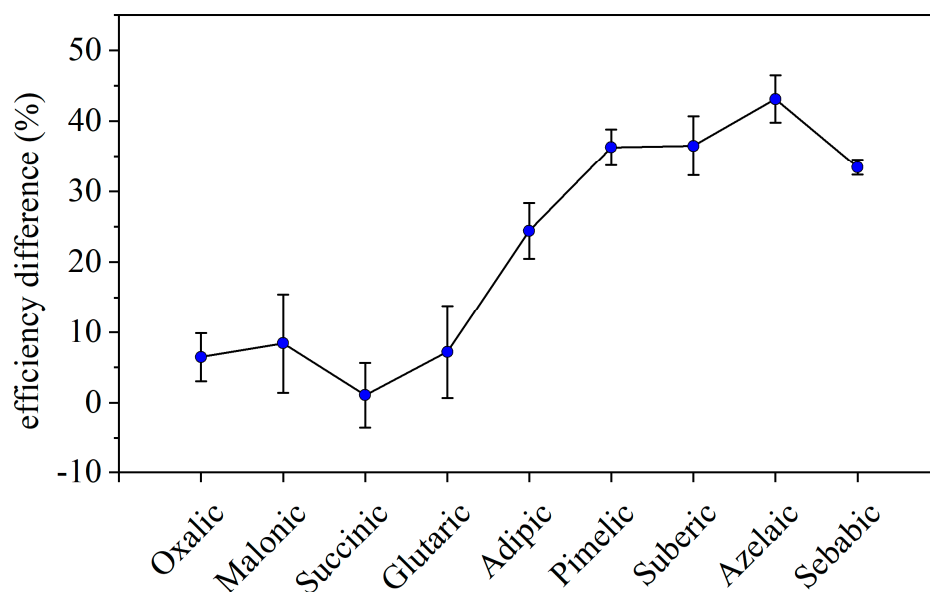


Figure S2. Differences in concentrations of particulate diacids measured by extraction with 50% methanol/water solution (v/v) compared to 100% water.

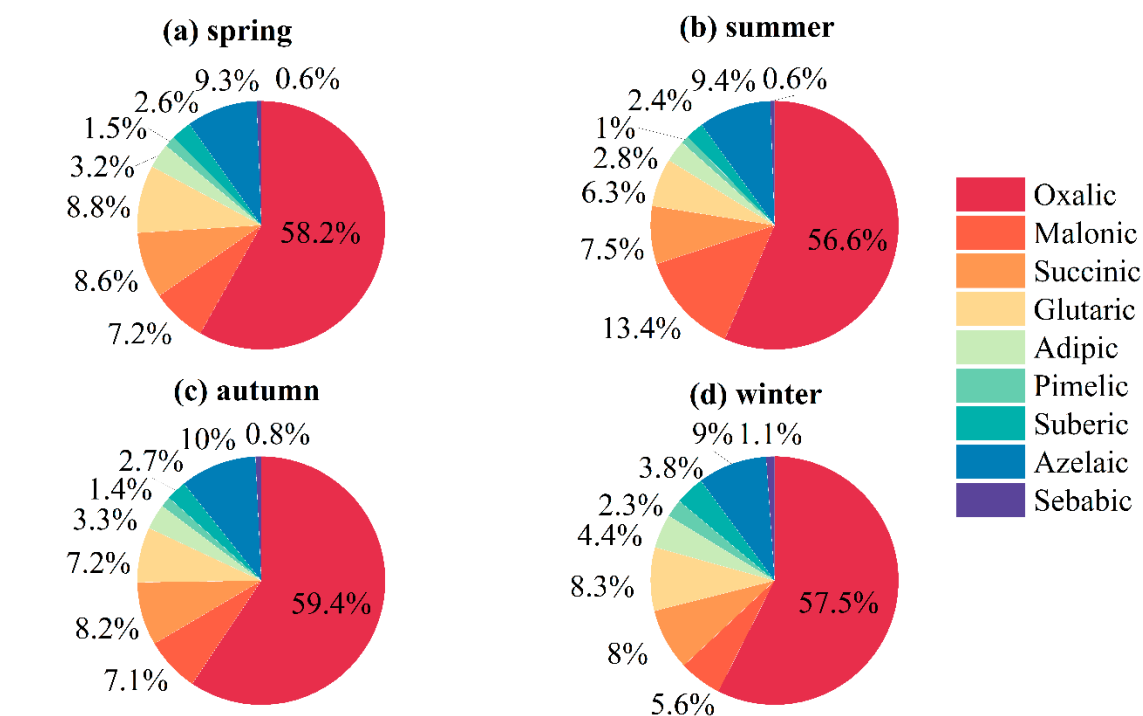


Figure S3. Seasonal variation of the diacid content in PM_{2.5} at the BS site.

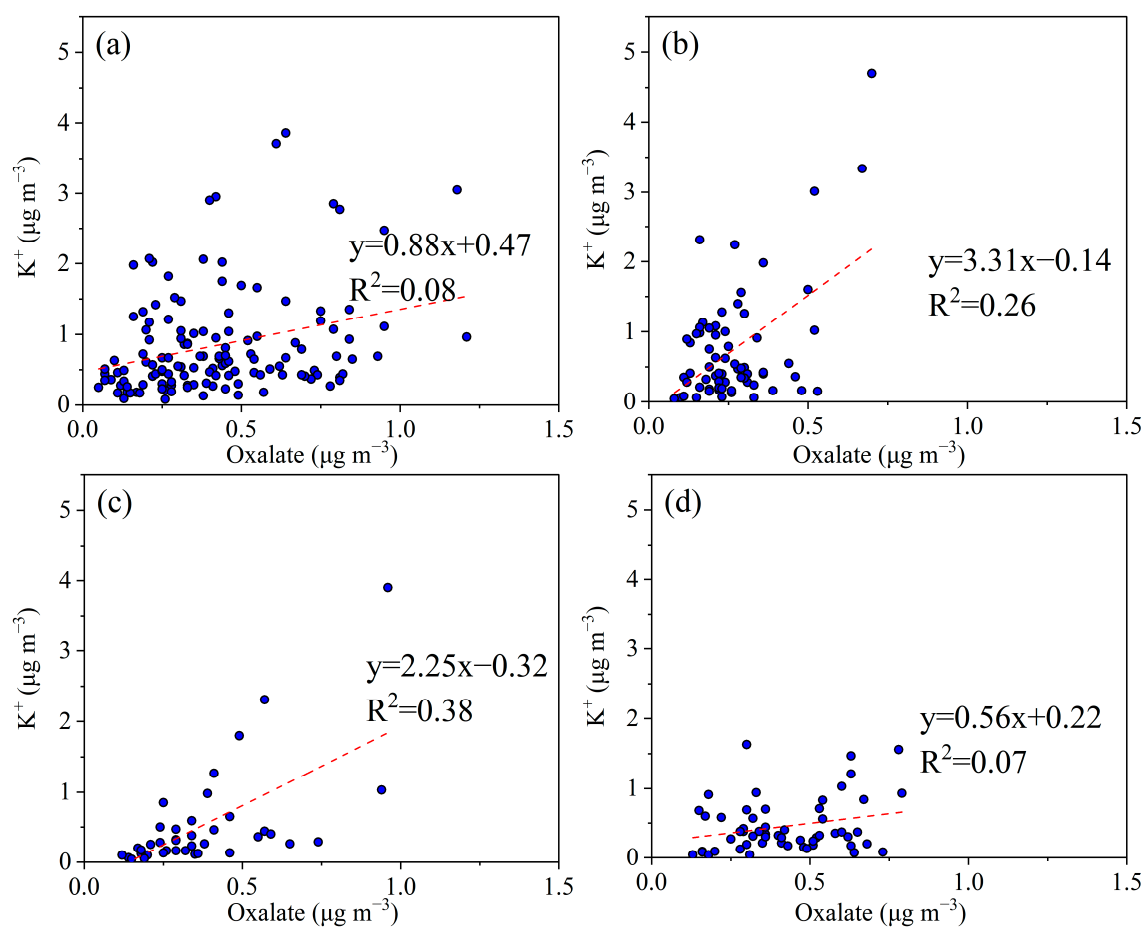


Figure S4. Correlation between oxalate and K^+ in (a):2008; (b):2010; (c):2013; (d):2014 at the BS site.

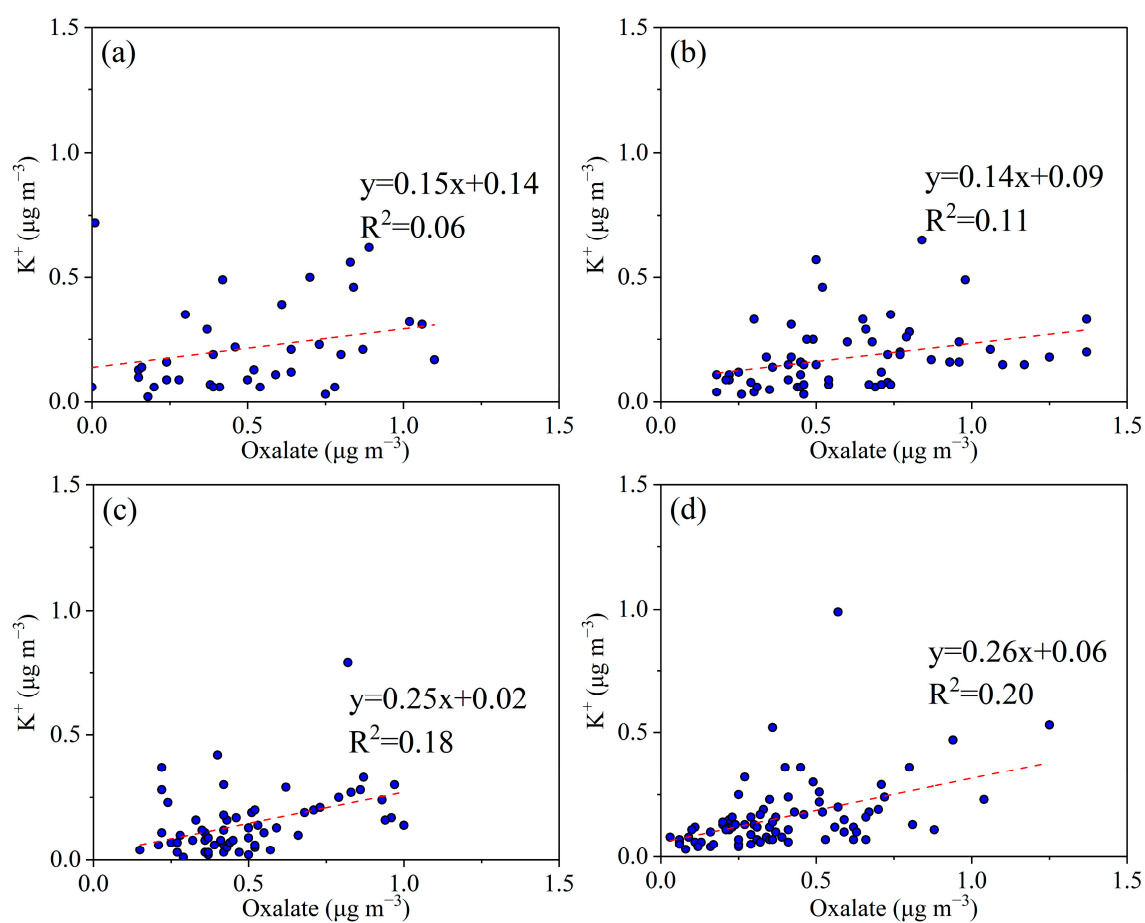


Figure S5. Correlation between oxalate and K^+ in (a):2016; (b):2017; (c):2018; (d):2019 at the PD site.

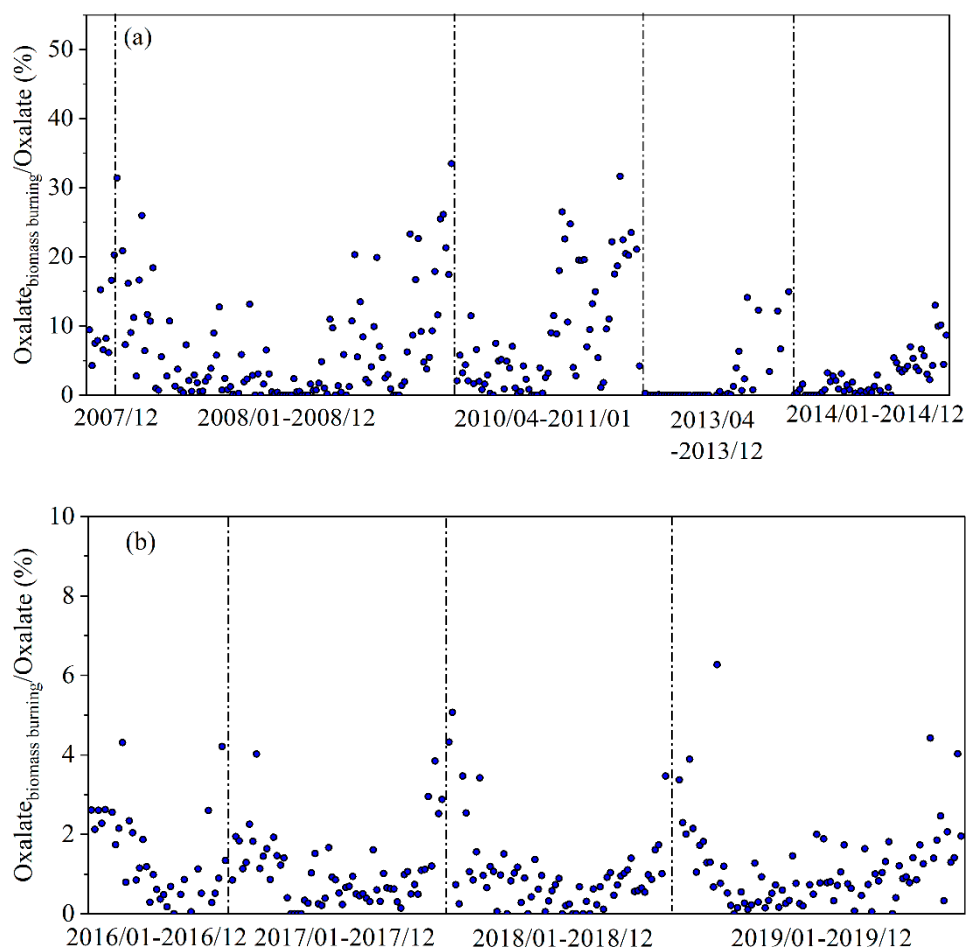


Figure S6. Time series of BB contribution to oxalate in BS (a) and PD (b).

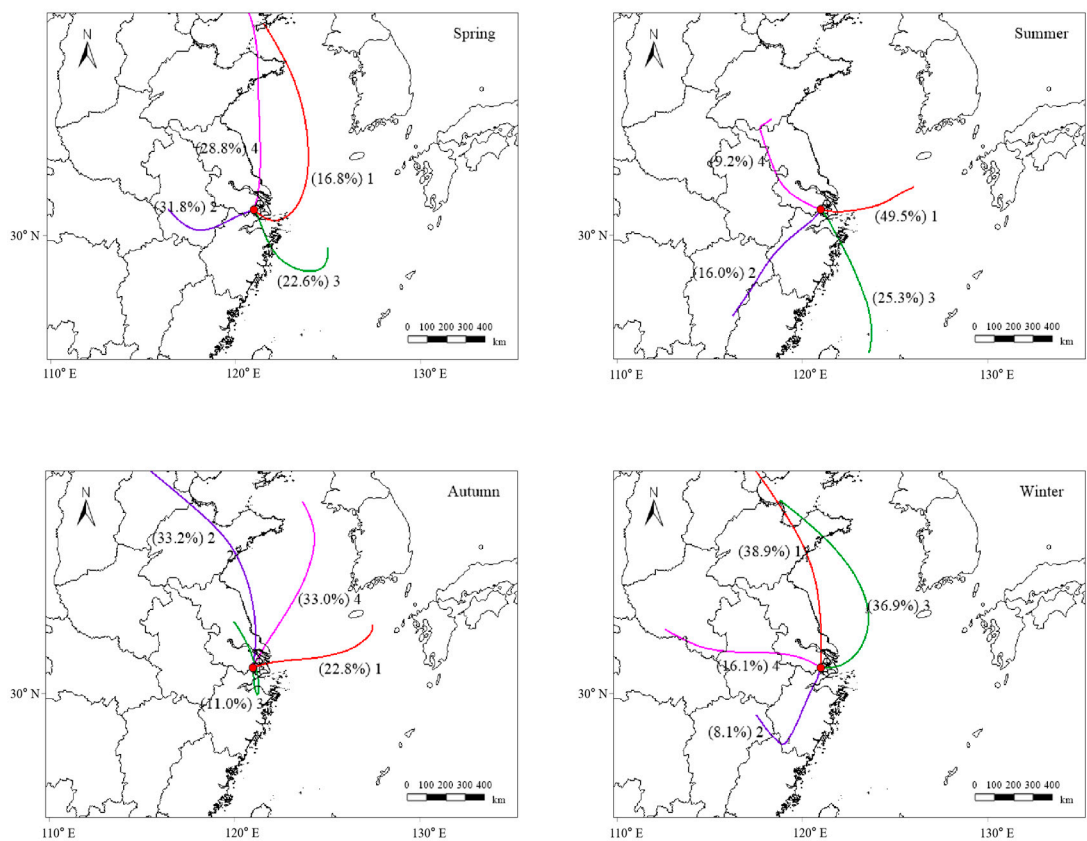
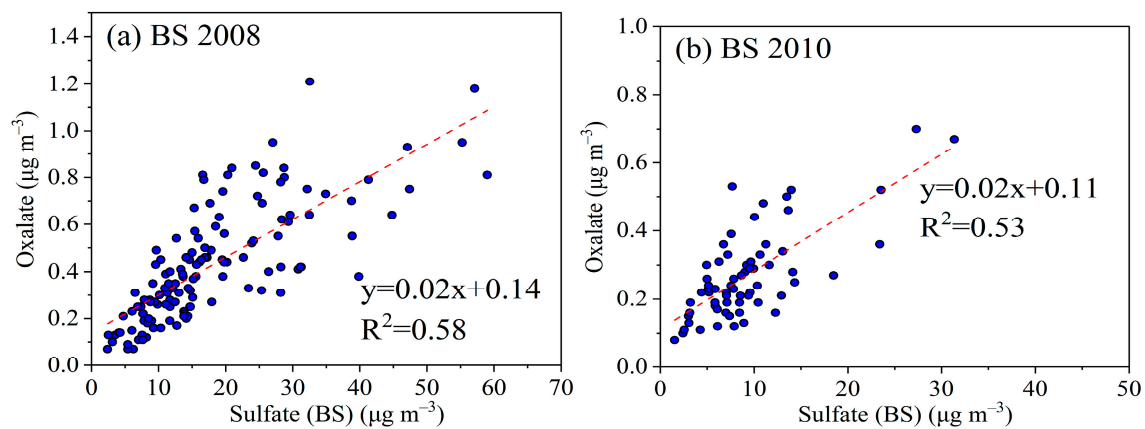


Figure S7. Clusters of backward trajectories for air parcels arriving in Shanghai during 2019.



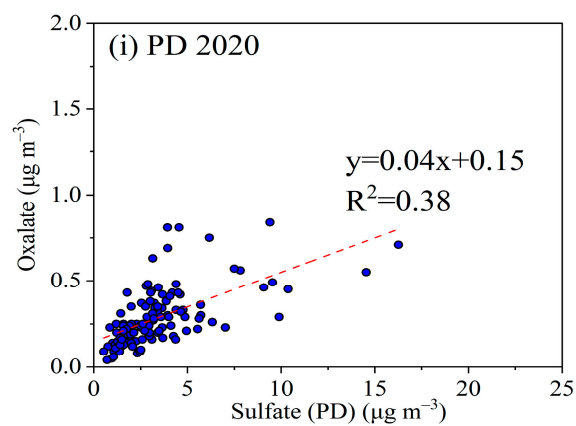
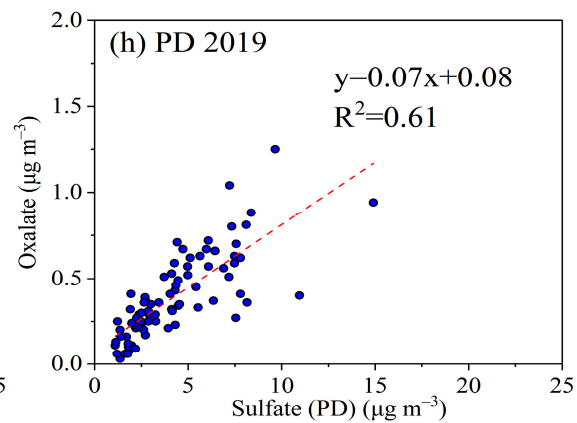
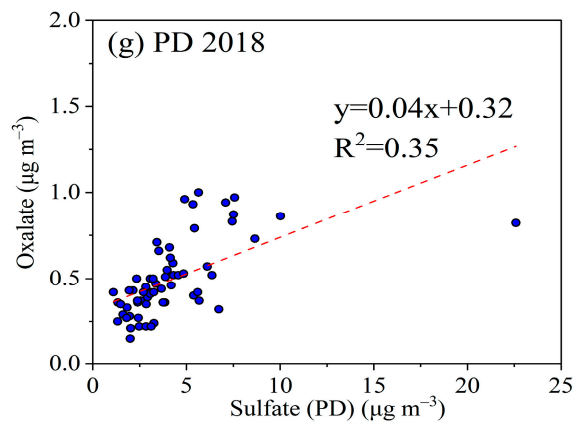
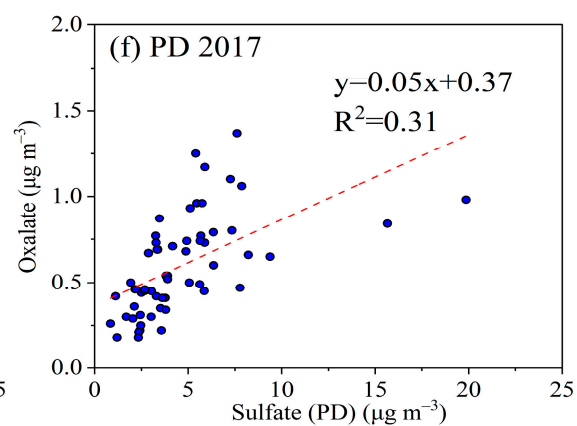
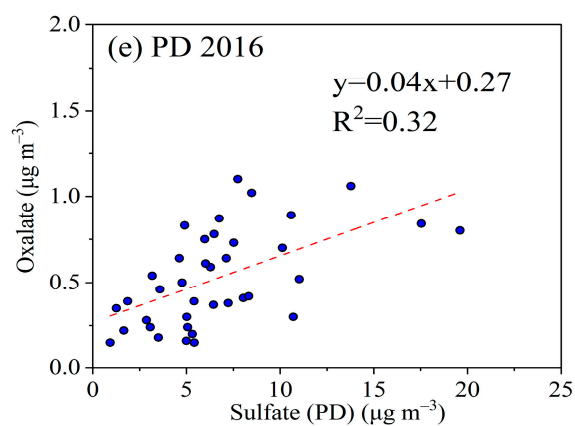
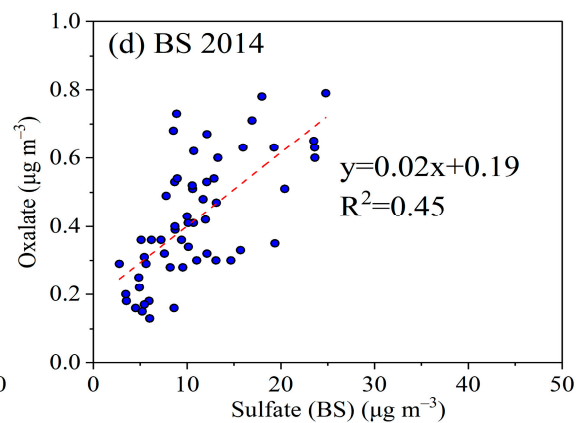
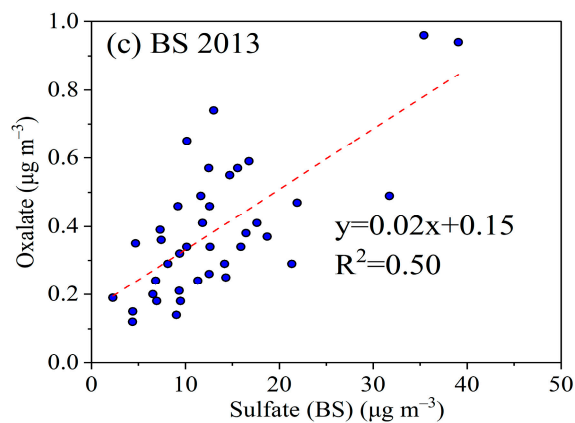
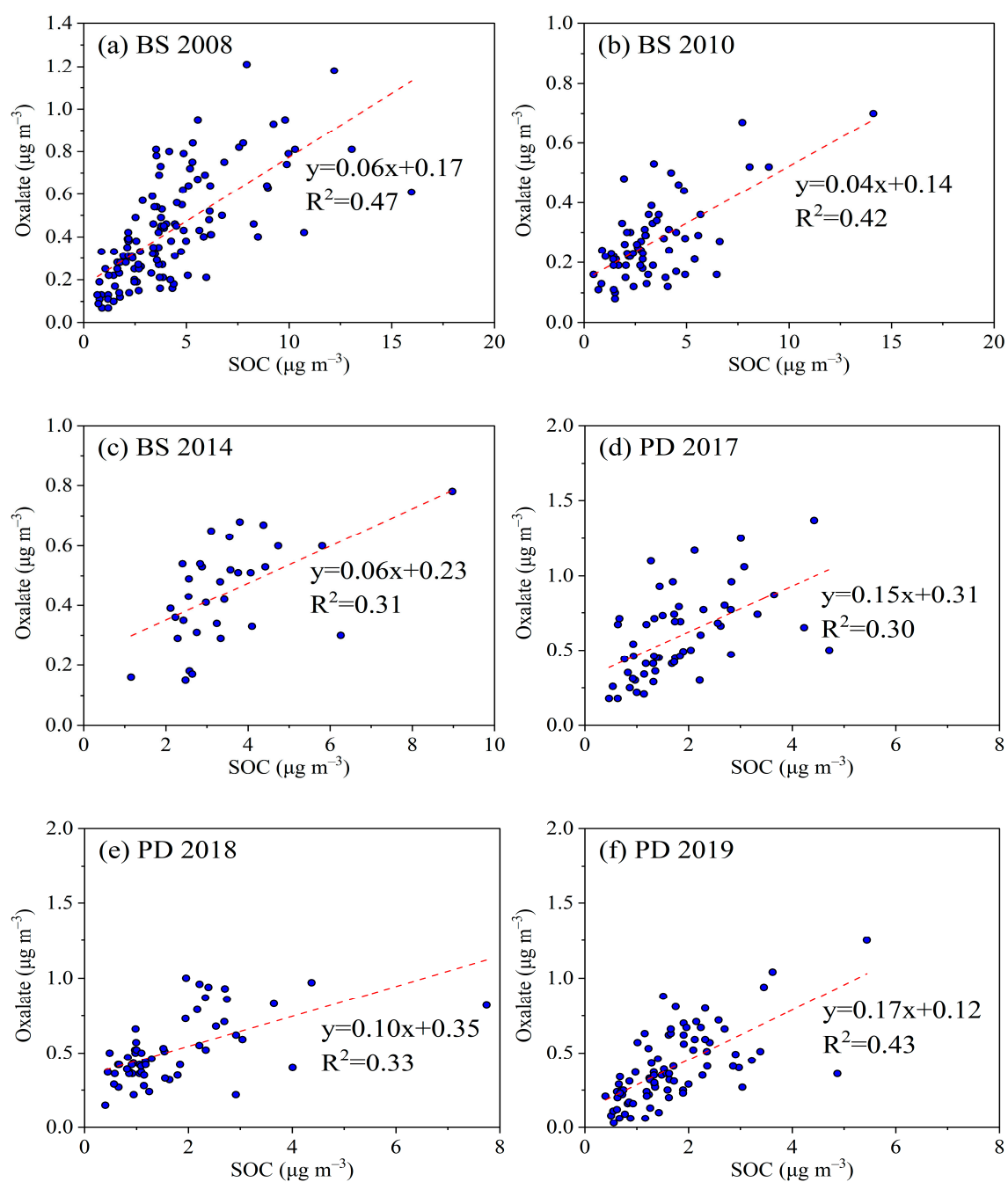


Figure S8. Oxalate correlation with sulfate: (a-i:BS2008-PD2020).



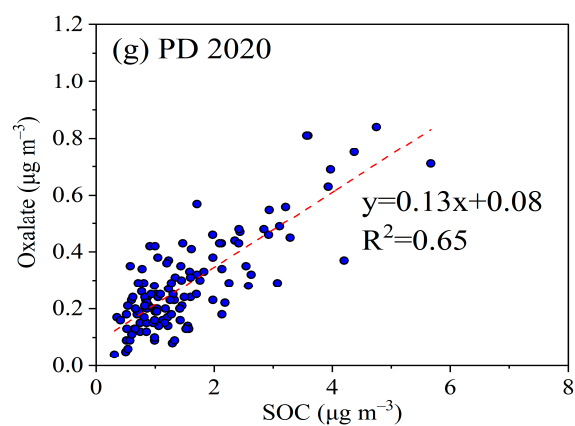
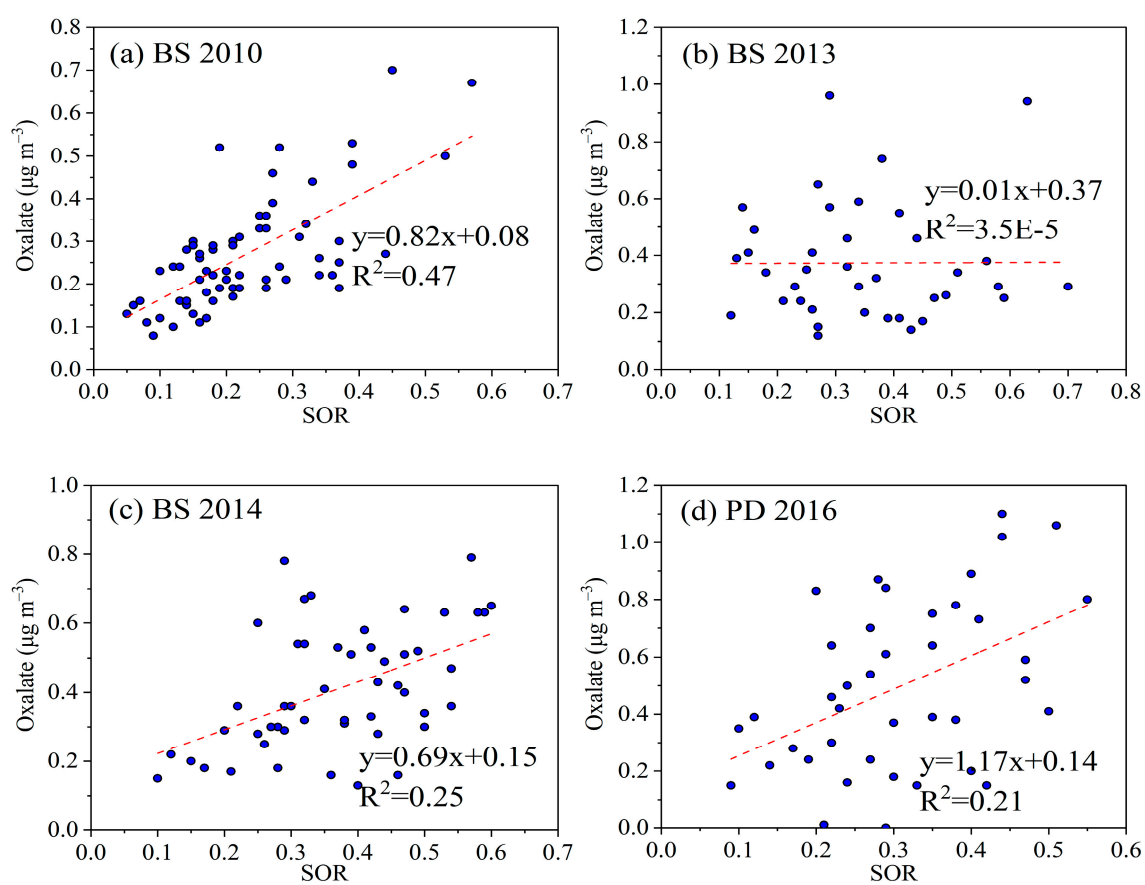


Figure S9. Oxalate correlation with SOC (a-g:BS2008-PD2020).



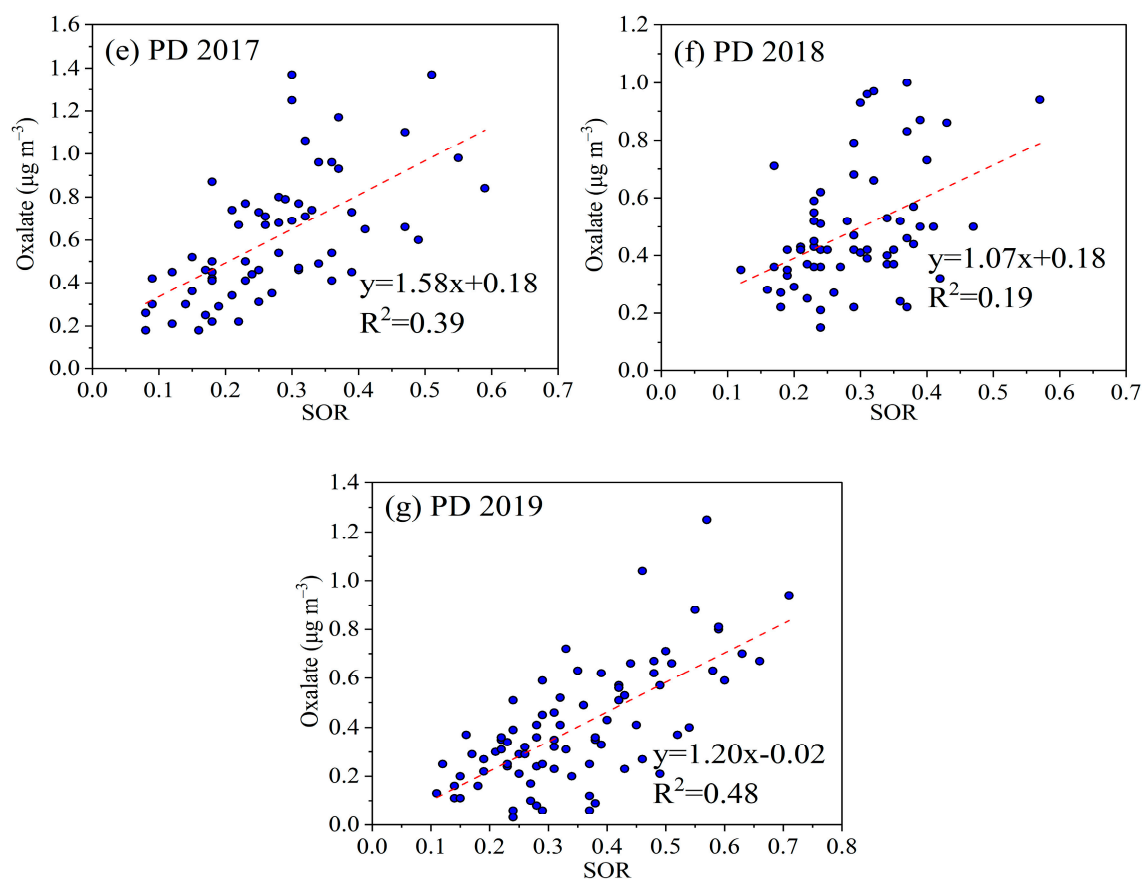


Figure S10. Oxalate correlation with SOR (a-g:BS2010-PD2019).

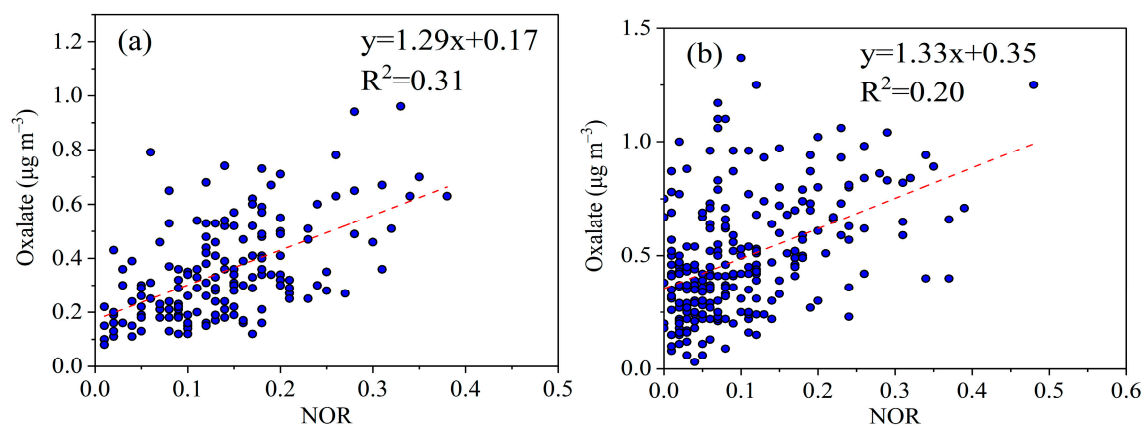


Figure S11. Oxalate correlation with NOR for BS (a) and PD(b).

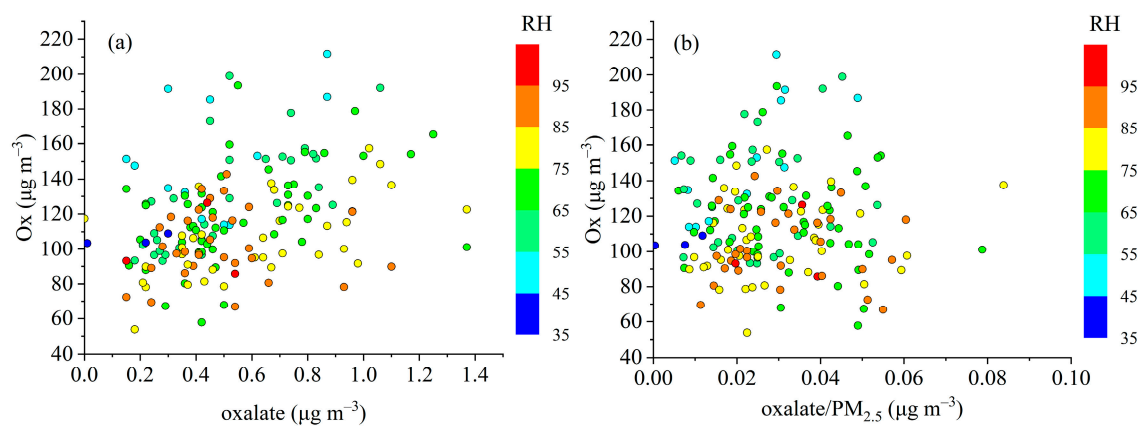


Figure S12. (a) RH distribution of oxalate and Ox; (b) RH distribution of oxalate/PM_{2.5} and Ox.

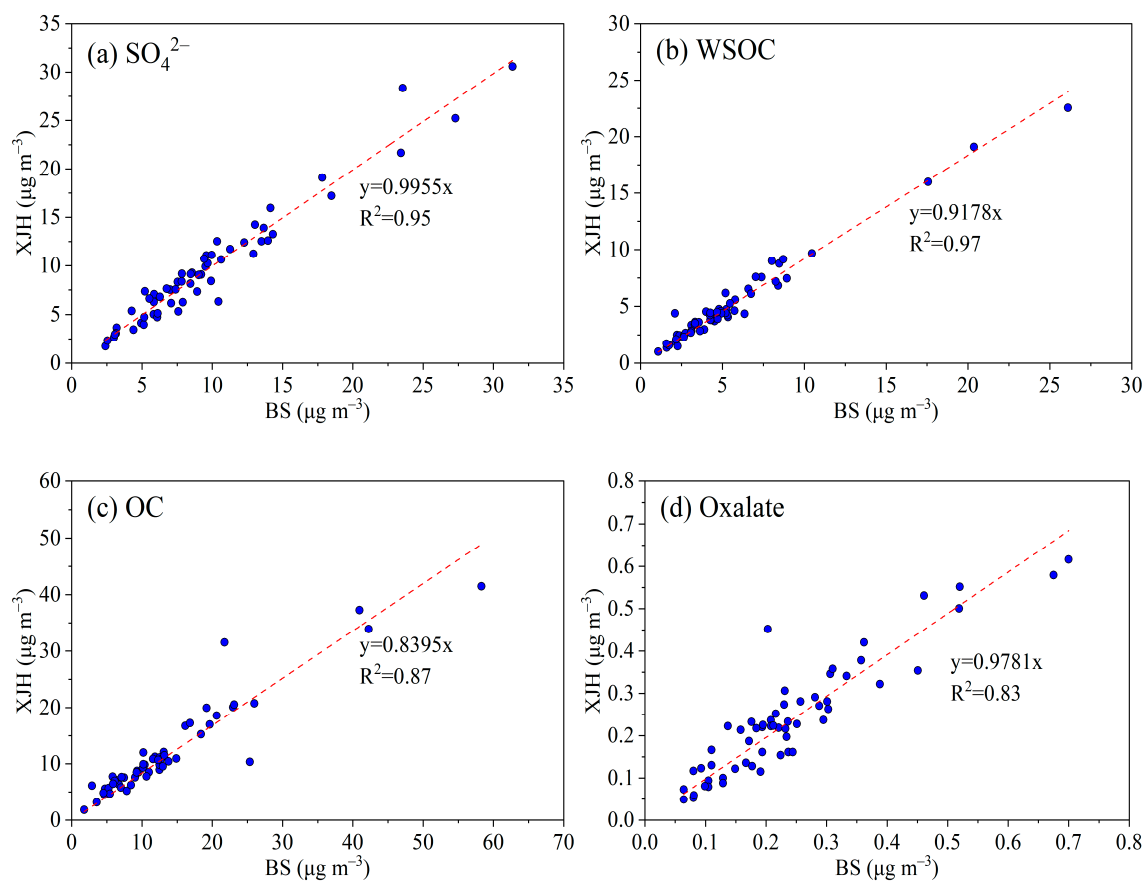


Figure S13. pollutants correlation in BS and XJH.

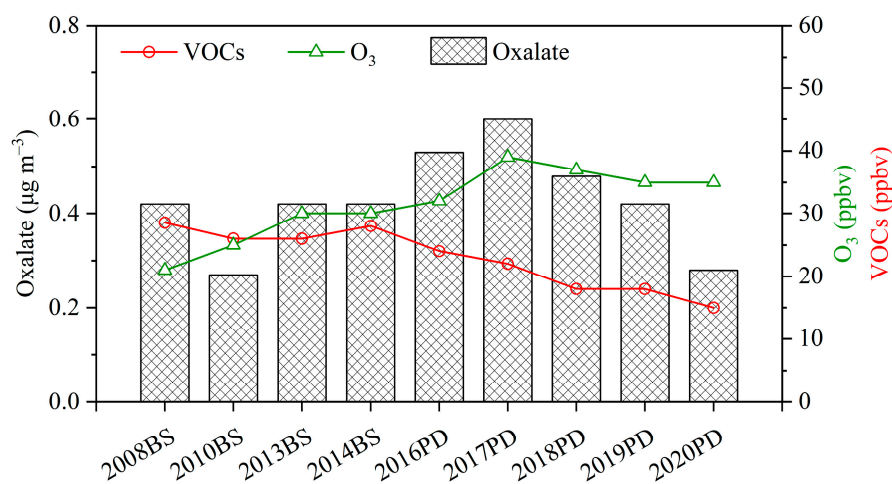


Figure S14. Interannual variation of the concentrations of oxalate, VOCs and O₃ in Shanghai (Data of VOCs of 2008-2014 was from Peng et al [1,2]; and VOCs of 2016-2020 and O₃ were from the Shanghai environmental monitoring center.).

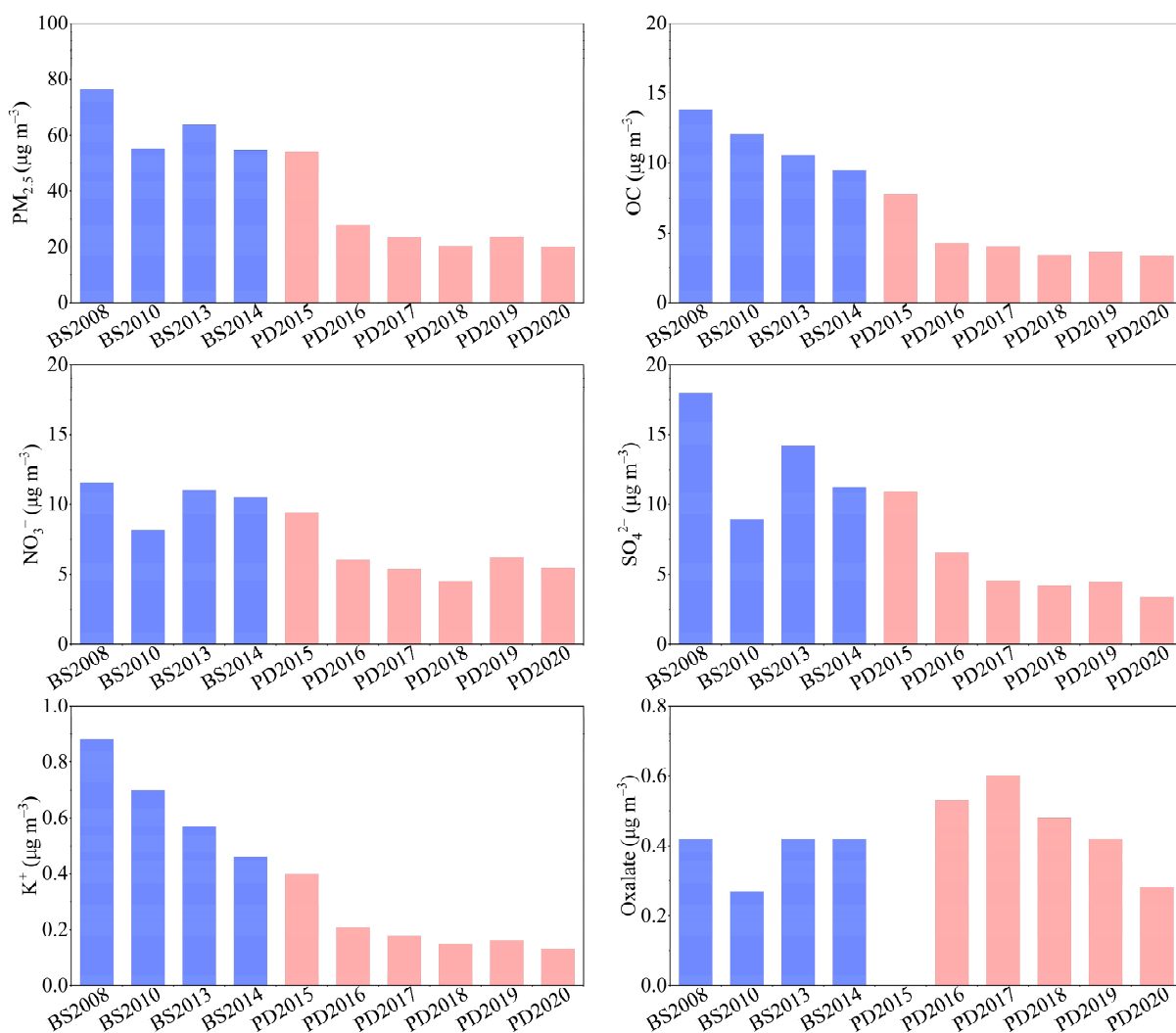


Figure S15. Evolution of particulate pollutants for Shanghai from 2008 to 2020. Blue bars represent BS and red bars represent PD.

Table S1. The ratio of Ca²⁺/K⁺ in biomass burning aerosol reported in previous studies.

| Sampling | Biomass type | Year | Region | K ⁺ (mg kg ⁻¹) | Ca ²⁺ (mg kg ⁻¹) | Ca ²⁺ /K ⁺ | References |
|----------|--------------|---------------|----------|---------------------------------------|---|----------------------------------|------------|
| Chamber | Corn cob | 2018.8-2019.2 | Liaoning | 174.66±46.01 | 18.47±2.14 | 0.11 | [3] |
| Chamber | Corn cob | 2018.8-2019.2 | Shanxi | 254.70±41.23 | 4.03±0.57 | 0.02 | [3] |
| Chamber | Corn cob | 2018.8-2019.2 | Henan | 208.17±53.47 | 44.92±34.51 | 0.22 | [3] |
| Chamber | Corn cob | 2018.8-2019.2 | Shandong | 540.73±95.65 | 12.21±4.49 | 0.02 | [3] |
| Chamber | Corn cob | 2018.8-2019.2 | Hubei | 269.02±45.58 | 22.31±11.15 | 0.08 | [3] |
| Chamber | Wheat straw | | | 530±250 | 82±72 | 0.15 | [4] |
| Chamber | Rice straw | | | 900±870 | 77±30 | 0.09 | [4] |
| Chamber | Corn straw | | | 280±120 | 88±43 | 0.31 | [4] |
| Chamber | Wheat straw | | | 350±180 | 30±20 | 0.09 | [5] |
| Chamber | Corn straw | | | 390±210 | 60±40 | 0.15 | [5] |
| Chamber | Rice straw | | | 390±280 | 30±10 | 0.08 | [5] |
| Chamber | Wheat straw | | | 490.21±359.74 | 19.35±75.43 | 0.04 | [6] |
| Chamber | Corn straw | | | 134.80±84.31 | 60.54±52.64 | 0.45 | [6] |
| Chamber | Rice straw | | | 246.10±297.61 | 65.79±60.95 | 0.27 | [6] |

Table S2. Annual PM_{2.5} concentrations at 9 monitoring stations in Shanghai during 2015-2021.

| Site | Huangpu | Hongkou | Xujiahui | Yangpu | Qingpu | Jing'an | Chuansha | PudongN | Zhangjiang | Baoshan | Average | CV |
|------|---------|---------|----------|--------|--------|---------|----------|---------|------------|---------|---------|------|
| 2015 | 55 | 52 | 53 | 54 | 63 | 55 | 50 | 52 | 51 | 56 | 54 | 6.7% |
| 2016 | 48 | 45 | 44 | 46 | 53 | 49 | 40 | 44 | 47 | 46 | 46 | 7.1% |
| 2017 | 38 | 40 | 38 | 39 | 39 | 44 | 40 | 36 | 37 | 40 | 39 | 5.3% |
| 2018 | 36 | 35 | 37 | 37 | 42 | 35 | 34 | 34 | 36 | 34 | 36 | 6.4% |
| 2019 | 34 | 35 | 37 | 37 | 37 | 38 | 35 | 34 | 34 | 36 | 36 | 4.0% |
| 2020 | 33 | 32 | 33 | 32 | 36 | 32 | 30 | 30 | 32 | 33 | 32 | 5.1% |
| 2021 | / | 28 | 29 | 27 | 29 | 29 | 26 | 28 | 29 | 28 | 28 | 3.1% |

References

- Peng, Y.; Wang, H.; Wang, Q.; Jing, S.; An, J.; Gao, Y.; Huang, C.; Yan, R.; Dai, H.; Cheng, T. Observation-based sources evolution of non-methane hydrocarbons (NMHCs) in a megacity of China – Science Direct. *J. Environ. Sci. (China)*. **2022**, *124*, 794–805.
- Xu, J.; Tie, X.; Gao, W.; Lin, Y.; Fu, Q. Measurement and model analyses of the ozone variation during 2006 to 2015 and its response to emission change in megacity Shanghai, China. *Atmos. Chem. Phys.* **2019**, *19*, 9017–9035.
- Wu, J.; Kong, S.; Yan, Y.; Yao, L.; Yan, Q.; Liu, D.; Shen, G.; Zhang, X.; Qi, S. Neglected biomass burning emissions of air pollutants in China-views from the corn cob burning test, emission estimation, and simulations. *Atmos. Environ.* **2022**, *278*.
- Ni, H.; Tian, J.; Wang, X.; Wang, Q.; Han, Y.; Cao, J.; Long, X.; Chen, L.; Chow, J.C.; Watson, J.G. PM_{2.5} emissions and source profiles from open burning of crop residues. *Atmos. Environ.* **2017**, *169*, 229–237.
- Zhang, H.; Hu, J.; Qi, Y.; Li, C.; Chen, J.; Wang, X.; He, J.; Wang, S.; Hao, J.; Zhang, L. Emission characterization, environmental impact, and control measure of PM_{2.5} emitted from agricultural crop residue burning in China. *J. Cleaner Prod.* **2017**, *149*, 629–635.
- Tian, J. Study on Emission Characteristics of PM_{2.5} from Crop Residue Burning and Residential Coal Combustion in China. Ph.D. Thesis, University of Chinese Academy of Sciences, Xi'an, China. October **2016**. Available online: (accessed date: 5 July 2020)